CHEMISTRY
A EUROPEAN JOURNAL

DOI: 10.1002/chem.200701850

Gold-Nanorod-Based Sensing of Sequence Specific HIV-1 Virus DNA by Using Hyper-Rayleigh Scattering Spectroscopy

Gopala Krishna Darbha, Uma Shanker Rai, Anant Kumar Singh, and Paresh Chandra Ray*[a]

Abstract: Infectious diseases caused by the human immunodeficiency virus (HIV) remain the leading killers of human beings worldwide, and function to destabilize societies in Africa, Asia, and the Middle East. Driven by the need to detect the presence of HIV viral sequence, here we demonstrate that the second-order nonlinear optical (NLO) properties of gold nanorods can be used for screening HIV-1 viral DNA sequence without any modification, with good sensitivity (100 picomolar) and selectivity (single base-pair mismatch). The hyper-Rayleigh scattering (HRS) intensity increases 45 times when a label-free 145-mer, ss-*gag* gene DNA, was hybridized with 100 pM target DNA. The mechanism of HRS intensity change has been discussed with experimental evidence for higher multipolar contribution to the NLO response of gold nanorods.

Keywords: DNA · gold · human immunodeficiency virus · nanostructures · sensors

Introduction

Infectious diseases remain the leading killers of human beings worldwide, and function to destabilize societies in Africa, Asia, and the Middle East. Acquired immunodeficiency syndrome (AIDS), a degenerative disease of the immune system, is caused by the human immunodeficiency virus (HIV). The current statistics for global HIV/AIDS are staggering, as an estimated 40 million people worldwide are ailing with HIV/AIDS. Diagnosis of the HIV infection is commonly based on the detection of antibodies to HIV, but generation of specific HIV antibodies usually occurs 3–8 weeks after the infectious contact and 5–10 days after the onset of symptoms associated with early infection. Despite infection of nearly 40 million individuals worldwide with HIV, fewer than 1000 cases have been diagnosed in the first month of infection, primarily because of the lack of a specific and recognizable acute retroviral syndrome. There is need for a direct DNA-based test that detects the presence of the HIV viral sequence. The nanoscience revolution that sprouted throughout the 1990s is having great impact in current and future DNA detection technology around the world.[1–12] The increasing availability of nanostructures with highly controlled optical properties in the nanometer size range has created widespread interest in their use in biotechnological systems for diagnostic application and biological imaging. Nanosurface fluorescence energy transfer (NSET)[13–16] and surface enhanced Raman spectroscopy (SERS) [17–20] have been shown to be highly promising technologies to detect DNA present at very low concentrations. However, these assays identify a specific sequence through hybridization of an immobilized probe to the target analyte after the latter has been modified with a covalently linked label such as a fluorescent or Raman tag. Necessity of tagging makes it difficult to use SERS and fluorescence resonance energy transfer (FRET) techniques as biosensors for real life. Diagnosis of an oligonucleotide sequence by using unmodified DNA remains attractive due to the simple sample preparation, low DNA assay cost, and the elimination of potential artifacts from modification. Driven by the need, we demonstrate for the first time that second-order nonlinear optical (NLO) properties[21–27] of gold nanorods can be used for screening HIV DNA without any modification, with excellent sensitivity (100 pM) and selectivity (single base-pair mismatch).

Gold nanosystems have created widespread interest in their use in biotechnological systems for diagnostic applications and biological imaging because of their shape and size-dependent optical properties, the origin of which is localized

[a] G. K. Darbha, Dr. U. S. Rai, Dr. A. K. Singh, Dr. P. C. Ray
Department of Chemistry
Jackson State University, Jackson, MS (USA)
Fax: (+1) 601-979-3674
E-mail: paresh.c.ray@jsums.edu

surface plasmon resonance (LSPR) and ease of bioconjugation and potential noncytotoxicity.[1–7] Conjugates of gold nanoparticles with oligonucleotides are of great current interest,[1–20] because of the potential use of the programmability of DNA base pairing to organize nanocrystals in space and the multiple ways of providing a signature for the detection of a precise DNA sequence. After a pioneering work by Mirkin et al.[28] several groups[1–20] including our group[6,14,16] are working in this area using different methods. The absorption spectra of rod-shaped gold nanoparticles, known as gold nanorods, exhibits two surface plasmon absorption bands.[8–12] A strong, long-wavelength band in the near-infrared region is due to the longitudinal oscillation of the conduction band electrons, and a weak, short-wavelength band around 520 nm is due to the transverse electronic oscillations. The longitudinal absorption band is very sensitive to the aspect ratio and by increasing the aspect ratio (length divided by width), the longitudinal absorption maximum shifts to longer wavelength with an increase in the absorption intensity. Because of the enhanced surface electric field, upon surface plasmon excitation the gold nanorods absorb and will be able to scatter electromagnetic radiation strongly. This unique optical property of gold nanorods opens up fascinating applications in biological and chemical sensors. Gold nanorods should provide several advantages over spherical gold nanoparticles for biological sensing: 1) the LSPR properties of gold nanorods can be tuned by adjusting their aspect ratio from the visible to the NIR region and 2) the longitudinal absorption band is extremely sensitive to changes in the dielectric properties of the surroundings, including solvents, adsorbates, and the interparticle distance of the gold nanorods. In this manuscript, we reported extremely high second-order nonlinear optical properties (NLO) of gold nanorods due to the presence of multipole moments from the size and retardation effects. NLO properties have been monitored by using the hyper-Rayleigh scattering (HRS) technique.[6,21–27] Using these enhanced, sensitive, and tunable optical scattering properties, we have shown that with the HRS technique,[6,21–27] which has emerged over the past decade as a powerful method to determine the microscopic nonlinear optical (NLO) properties of species in solution, we can achieve detection of HIV DNA with excellent sensitivity (100 pM) and selectivity (single base-pair mismatch).

Experimental Section

Synthesis and characterization of gold nanorods: Gold nanorods were synthesized by using a seed-mediated, surfactant-assisted growth method in a two-step procedure.[8–12,29–34] Colloidal gold seeds ($\approx$1.5 nm diameter) were first prepared by mixing aqueous solutions of hexadecylcetyltrimethylammonium bromide (CTAB, 0.1 M, 4.75 mL) and hydrogen tetrachloroaurate(III) hydrate (0.01 M,.2 mL). An aqueous solution of sodium borohydride (0.01 M, .6 mL) was then added. These colloidal gold seeds were then injected into an aqueous growth solution of CTAB (0.1 M, 4.75 mL), silver nitrate (0.01 M, varying amounts of silver between 20 and 120 mL depending on desired nanorod aspect ratio), hydrogen tetrachloroaurate(III) hydrate (0.01 M, 0.2 mL), and ascorbic acid (0.1 M, .032 mL). The nanorods were purified by several cycles of suspension in ultrapure water, followed by centrifugation. They were isolated in the precipitate, and excess CTAB was removed in the supernatant. The nanorods were characterized by TEM and absorption spectroscopy (as shown in Figure 1).

Preparation of DNA gold nanorod conjugates: The nanorods prepared by above methods were capped with a bilayer of cetyltrimethylammonium bromide (CTAB), which is positively charged. The positively charged

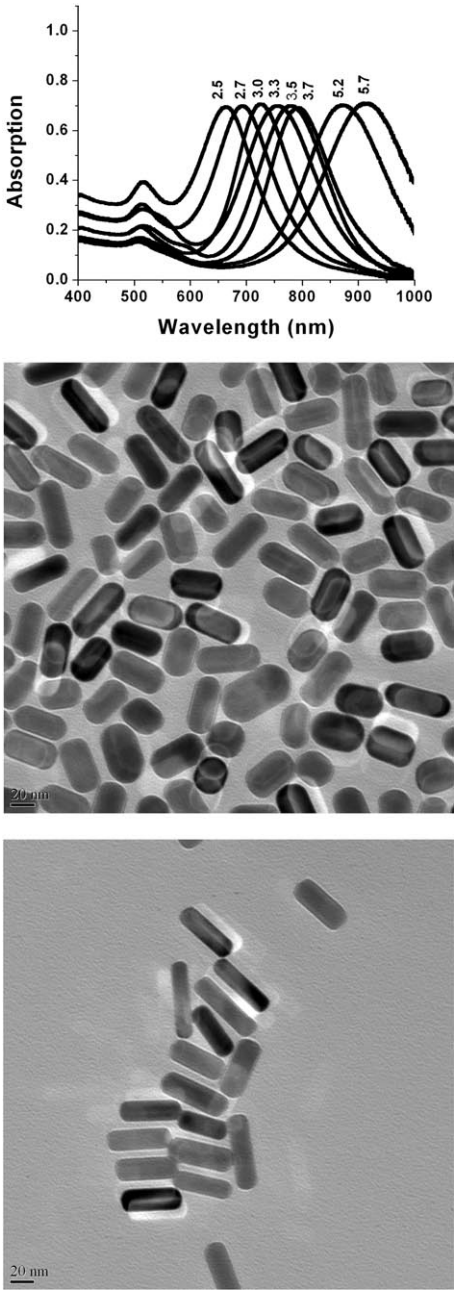

Figure 1. Top: Extinction profile of Au nanorods with aspect ratios from 2.5 to 5.7. The strong long wavelength band in the near-infrared region (λ_{LPR} = 600–950 nm) is due to the longitudinal oscillation of the conduction band electrons. The short wavelength peak ($\lambda \approx$ 520 nm) is from the nanorods' transverse plasmon mode. Below: TEM images of nanorods of average aspect ratios (σ) $\approx$2.5 (middle) and 3.3 (bottom); bars represent 20 nm.

surface of the nanorods was changed to a negatively charged surface by exposing the nanoparticles to poly(styrenesulfonate) (PSS) polyelectrolyte solution. The extra PSS in solution was separated by centrifuging the rod solution at 8000 rpm, and the pellet was redispersed in *N*-(2-hydroxyethyl)piperazine-*N*′-2-ethanesulfonic acid (HEPES) solution. The PSS-capped nanorods were then mixed with probe DNA solution that was diluted in buffer and allowed to react for 20 min. The probe DNA was probably bound to the PSS-coated nanorods by a mechanism similar to that used for binding DNA to nanospheres, that is, by electrostatic physisorption interaction.[14,16,35,6] Direct evidence for the preferential interaction between dye-tagged ssDNA and gold nanoparticles is illustrated in Figure 2. Our experimental data showed quenching of the dye photoluminescence from dye-tagged ssDNA and enhancement of resonant Raman

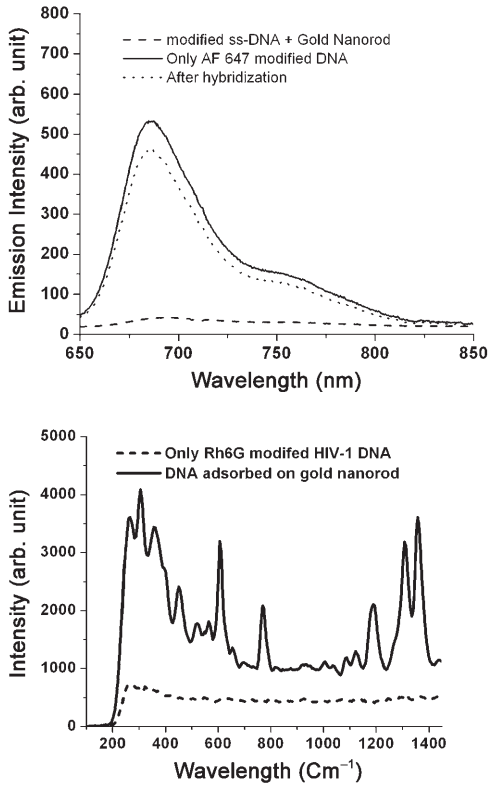

Figure 2. Top: Fluorescence emitted from from AlexaFluor 647 (AF647) modified to ssDNA (AF647–5′-AGAAGATATTTGGAATAACATGACCTGGATGCA-3′) was quenched by more than 95% by gold nanorods. Upon hybridization, the double-stranded (ds)-DNA is no longer absorbed onto the gold nanorods and the fluorescence of the dye persists. Bottom: Surface-enhanced resonant Raman scattering (SERRS) from rhodamine 6G-tagged ssDNA (Rh6G –5′-AGAAGATATTTGGAATAACATGACCTGGATGCA-3′) with and without gold nanorods.

scattering from the dye. Fluorescence emitted from AlexaFluor 647 (AF647)-modified ssDNA (AF647–5′-AGAAGATATTTGGAATAACATGACCTGGATGCA-3′) was quenched more than 95% by gold nanorod as shown in Figure 2 (top). The fluorescence spectra were recorded by using our NSET Probe as previously reported.[14,16,35] From surface-enhanced resonant Raman scattering (SERRS) measurements several orders of magnitude signal enhancement were observed (as shown in Figure 2, bottom) from rhodamine 6G (Rh6G)-tagged ssDNA (Rh6G –5′-AGAAGATATTTGGAATAACATGACCTGGATGCA-3′) adsorbed on gold nanorods. The Raman modes at 234, 253, 273, and 371 cm^{-1} are N-C-C bending modes of ethylamine group of the Rh6G ring and the strong Raman modes at 613, 777, 1182, 1347, and 1366 cm^{-1} are due to C-C-C ring in-plane bending, C–H out-of-plane bending, C–C stretching, and C–N strectching, respectively. Details of SERS measurements have been reported recently.[36]

Since certain regions of the *gag* gene, such as p24, are highly conserved among human immunodeficiency virus (HIV) isolates, many therapeutic strategies have been directed at *gag*-gene targets. We therefore used a segment of HIV *gag*-gene sequence as a target DNA. To demonstrate that HRS assay can be used for HIV-DNA detection, we initially used a partial sequence of the HIV-1 *gag* gene, 5′-AGAAGATATTTGGAATAACATGACCTGGATGCA-3′, as the probe. Then to understand the capability of our HRS assay for longer DNA sequences we used 86, 115 and 142 base pair (bp) fragments from the *gag* region. Oligonucleotides with different chain lengths, and its complement and noncomplement (one and two base pair mismatch), were purchased from the Midland Certified Reagent Company. Hybridization of the probe and the target was conducted for 5 min in phosphate buffer solution with 0.3 M NaCl for few minutes at room temperature. An aliquot of the hybridization solution was added to the gold nanorod solution (1 mL). Phosphate buffer (1 mL) was added immediately to the same solution.

Hyper-Rayleigh scattering (HRS) spectrosocpy: The HRS technique is based on light scattering. The intensity of the Rayleigh scattering is linearly dependent on the number density and the impinging laser intensity, and quadratically on the linear polarizability α. The HRS or nonlinear light scattering can be observed from fluctuations in symmetry, caused by rotational fluctuations. This is a second-harmonic-generation experiment in which the light is scattered in all directions rather than as a narrow coherent beam. The technique can be easily applied to study a very wide range of materials, because electrostatic fields and phase matching are not required.[6,21–26,37–40] Other advantages are that the polarization analysis gives information about the tensor properties, and spectral analysis of the scattered light gives information about the dynamics. We monitored the second-order NLO properties using the HRS technique. Scattering by a fundamental laser beam can be detected at the second harmonic wavelength. This is a second-harmonic-generation experiment in which the light is scattered in all directions rather than as a narrow coherent beam. For the HRS experiment, we used a mode-locked Ti:sapphire laser, delivering at fundamental wavelength of 860 nm with a pulse duration of about 150 fs at a repetition rate of 80 MHz. We performed TEM data (as shown in Figure 1, bottom) before and after exposure of about 5 min to the laser and we did not note any photothermal damage of gold nanorods within our HRS data colleting time. After passing through a low-pass filter, a fundamental beam of about 100 mW was focused into quartz cell containing the aqueous solutions of the metallic particles. The HRS light was separated from its linear counterpart by a 3 nm bandwidth interference filter and a monochromator and then detected with a cooled photomultiplier tube (PMT), and the pulses were counted with a photon counter. The fundamental input beam was linearly polarized, and the input angle of polarization was selected with a rotating half-wave plate. In all experiments reported, the polarization state of the harmonic light was vertical. Gold nanorods are known to possess strong two-photon luminescence (TPL).[19,41] To avoid TPL contributions from HRS signal, we used the following steps: 1) We used gold nanorods of aspect ratios 2.5 and 2.7, the λ_{max} of which was 200 nm away from the excitation wavelength. Our experiments indicate that in case of 860 nm excitation, TPL signal can be observed for nanorods with aspect ratio between 3.3–5.2. 2) We used a 3 nm interference filter in front of PMT, to make sure that only second-harmonic signal is collected by PMT.

Results and Discussion

NLO properties of gold nanorods and evidence for multipoles: To understand whether the two-photon scattering intensity at 430 nm light is due to second-harmonic generation, we performed power-dependent as well as concentration -dependent studies. Figure 3 shows the output signal in-

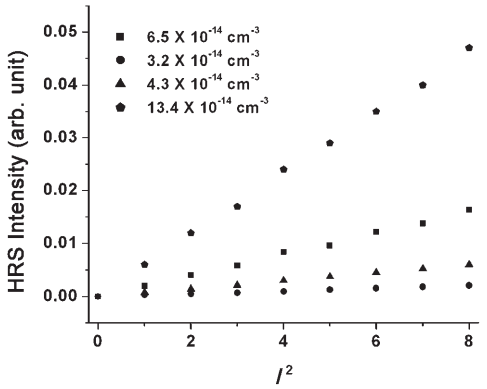

Figure 3. Power dependence of HRS intensity at different concentration of gold nanorods.

tensities at 430 nm from ss-DNA absorbed gold nanoparticles at different powers of 860 nm incident light. A linear nature of the plot implies that the doubled light is indeed due to the HRS signal.

Figure 4 shows $\log(I_{2\omega})$ versus $\log(I_{\omega})$ plot. A linear nature of the plot with slope 1.92 also supports that the

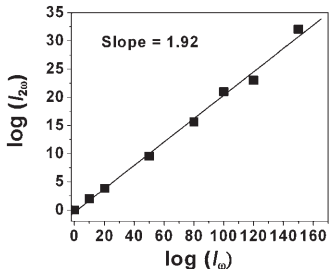

Figure 4. Excitation power dependence of the detected HRS signal from gold nanorod solution (excitation wavelength was 860 nm).

HRS signal is due to the second-harmonic light. The intensity I_{HRS} of the hyper-Rayleigh signal from an aqueous solution of gold nanorods can be expressed as Equation (1) in which G is a geometric factor, N_w and N_{nano} the number of water molecules and gold nanorods per unit volume, β_W and β_{nano} are the quadratic hyperpolarizabilities of a single water molecule and a single gold nanorod, $\varepsilon_{2\omega}$ is the molar extinction coefficient of the gold nanorod at 2ω, l is the path length, and I_{ω} the fundamental intensity. The exponential factor accounts for the losses through absorption at the harmonic frequency.

$$I_{HRS} = G\langle N_w\beta_w^2 + N_{nano}\beta_{nano}^2\rangle I_{\omega}^2 e^{-N_{nano}\varepsilon_{2\omega} l} \quad (1)$$

To extract absolute values of the hyperpolarizabilities, the normalized intensities were normalized again with *para*-nitroaniline (pNA) in methanol. By using $\beta_w = 0.56\times10^{-30}$ esu, as reported in the literature, we have found out $\beta_{nano} = 3.8\times10^{-24}$ esu for 80 nm gold nanorod and 4.2×10^{-24} esu for DNA adsorbed gold nanorod, which is about 3–4 orders of magnitude higher than the β values reported for the best available molecular chromophores[21–27,37] and 1–2 orders of magnitude higher than the β value reported for gold nanoparticles.[6,22,38,39] This higher β value for nanorods with respect to nanosphere can be due to several facts and these are 1) The presence of {110} facets, which is not present in nanospheres, is known to give rise to strong absorption energies; 2) the surface electromagnetic field of rods is the highest relative to other shapes due to the rod's high curvatures (called "the lightning rod" effect[40]); 3) the presence of multipoles; and 4) possibility of single-photon resonance enhancement. The optical responses of particles that are small compared to the wavelength can be described usually in the framework of electric-dipole approximation. However, when the particle size approaches the wavelength, the dipolar picture may no longer provide a complete description, and higher multipolar interactions should be considered. Multipoles can arise by two different ways: 1) from the light–matter interaction Hamiltonian, corresponding to microscopic multipole moments, and 2) according to Mie's scattering theory.[41] Standard Mie's theory is based on dipolar interactions, and multipoles arise from the size and retardation effects. Since there is a center of inversion in the nanorod, the HRS intensity arising from gold nanorod cannot be due to electric dipole contribution. At the microscopic scale, the breaking of the centrosymmetry is required for the harmonic generation process at the surface of the particle. Considering the size of a nanorod, the approximation that assumes that the electromagnetic fields are spatially constant over the volume of the particle is not suitable anymore. Higher orders of the electromagnetic field's spatial expansion must be incorporated into the description. As a result, the total nonlinear polarization consists of different contributions, such as multipolar radiation of the harmonic energy of the excited dipole and possibly of higher multipoles. The HRS intensity therefore also consists of several contributions. The first one is the electric-dipole approximation, which may arise due to the defects in nanorods. This contribution is actually identical to the one observed for any noncentrosymmetric pointlike objects, such as efficient rodlike push–pull molecules. This electric dipole nature presents two lobes oriented along the 0–180° axis. The second contribution is multipolar contribution like electric quadrupole contribution. This contribution is very important when the size of the particle is no longer negligible when compared to the wavelength.

This contribution pattern shows four lobes (as shown in Figure 5) oriented on the 45, 135, 225, and 315° axes when the vertically polarized harmonic output is considered. Figure 5 demonstrates the polar plots of the HRS intensity vertically polarized as a function of the angle of polarization of the fundamental incoming beam for two types of gold particles: 1) 20 nm diameter gold nanosphere, 2) 120×45 nm gold nanorods. Our experimental results show clearly four-lobe pattern for gold nanorods and two-lobe pattern for gold nanospheres. So our experimental results show that the origin of the very high HRS light is due to the presence of both dipolar and quadrupolar contributions. For our gold

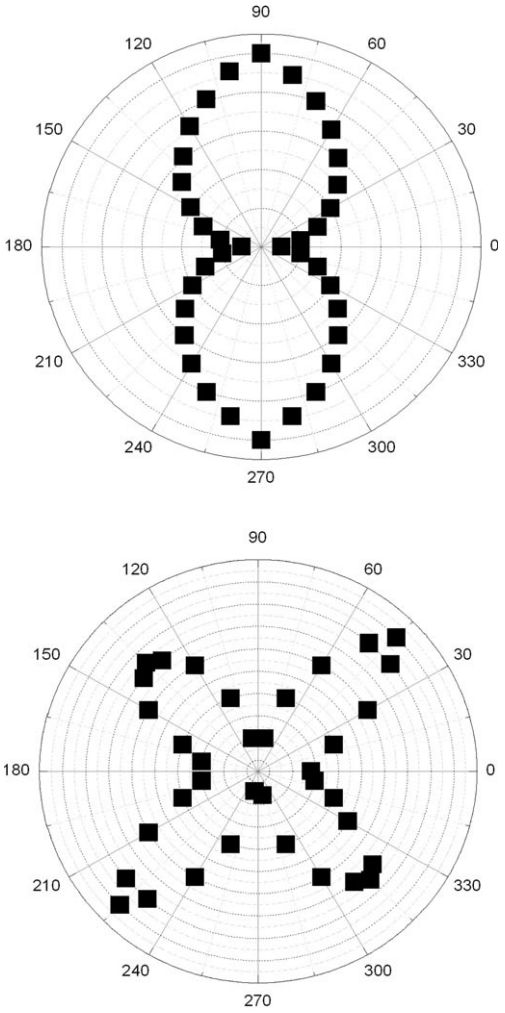

Figure 5. Polar plot of the HRS intensity as a function of the incoming fundamental beam polarization angle from aqueous suspensions of 20 nm gold spherical colloids (top) and 120×45 nm gold nanorods (bottom).

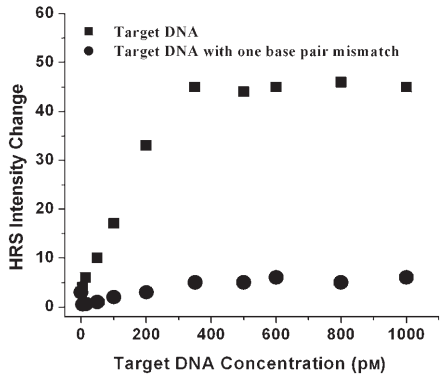

Figure 6. Plot of HRS intensity change versus target DNA {exact complementary of HIV-1 *gag* gene DNA (5′-AGAAGATATTTGGAATAA-CATGACCTGGATGCA-3′ and one base pair mismatch} concentration at the picomolar level.

nanoparticle, the ratio between the length of the particles and the wavelength of the fundamental beam is only 3/17, which is too large to neglect the retardation effect. This four-lobe pattern is not regular as demonstrated by the size inequality between the lobes. In particular, the lobes at 45 and 225° are larger than those collected at 135 and 315°. These deviations from the perfect polar plot are due to the retardation effects of the electromagnetic fields.

Sequence specific HIV-1 *gag* gene DNA diagnostics: Figure 6 shows how the HRS intensity varies after the addition of target DNA into probe HIV-1 *gag*-gene DNA (5′-AGAAGATATTTGGAATAACATGACCTGGATGCA-3′) (400 pM). We observed a very distinct HRS intensity change after hybridization even at the concentration of 100 picomolar probe ss-DNA. The HRS intensity changes only 10% when we added the target DNA with one base-pair mismatch with respect to probe DNA (as shown in Figure 6). Our detection is based on the fact that double- and single-stranded oligonucleotides have different electrostatic properties as shown in Scheme 1. When DNA is adsorbed onto the nanorod, due to conformationally flexible backbone of a single-stranded DNA, a favorable conformation for the adsorbed oligonucleotides is an archlike structure, in which

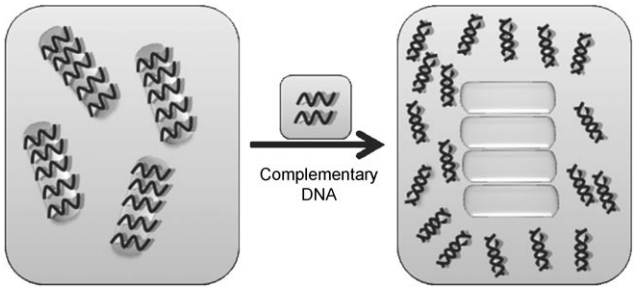

Scheme 1. Schematic representation of the gold-nanorod-based DNA hybridization process.

both the 3′- and 5′-ends are attached to the particle. Since the ds-DNA cannot uncoil sufficiently like ss-DNA to expose its bases toward the gold nanorods, repulsion between the charged phosphate backbone of ds-DNA and negatively charged ions from the gold nanorods surface dominates the electrostatic interaction, which does not allow ds-DNA to adsorb onto gold nanorods.

The fact that dye-tagged ssDNA adsorbs onto the gold, whereas dsDNA does not adsorb, can be seen through the effects of adding complementary DNA to solutions containing dye-tagged ssDNA adsorbed onto gold nanorods. Upon hybridization, the double-strand (ds) DNA is no longer adsorbed onto the gold nanorods and the fluorescence of the attached dye persists (as shown in Figure 2, top).

As soon as the ds-DNA separated from gold nanorod, a second effect, aggregation of gold nanorod has been observed as evidenced by TEM image (Figure 7), which has been further confirmed by absorption spectroscopic studies (Figure 8, top). This is due to the screening effect of the salt, which minimizes electrostatic repulsion between the oligo-

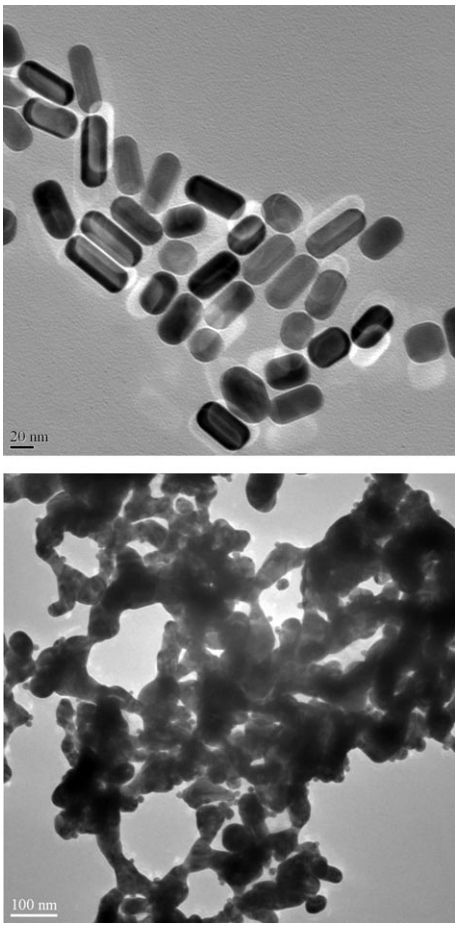

Figure 7. TEM images of nanorods before (top) and after (bottom) hybridization.

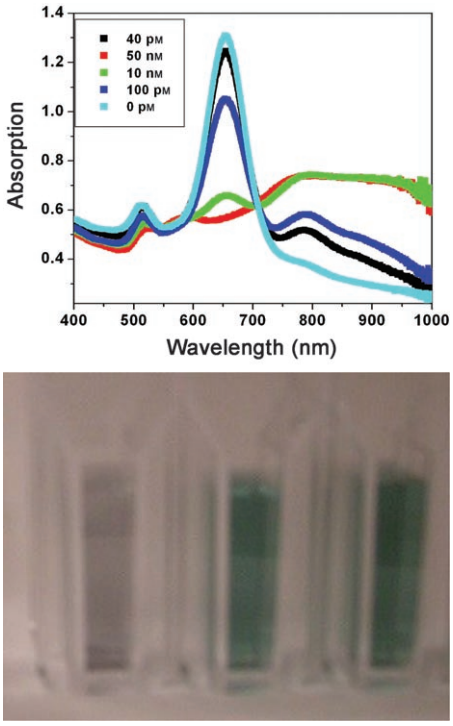

Figure 8. Top: Absorption profile of DNA coated Au nanorods before and after hybridization with different concentrations of probe DNA. Bottom: Colorimetric change upon addition of 10 nM (left), 100 pM (middle), and 0 pM (right) probe DNA.

nucleotide-modified particles, allowing more hybridization events to take place, leading to more linked particles and hence larger damping of the surface plasmon absorption of Au nanorod surfaces. We also note that though the HRS intensity changes by an order of 17 even at the concentration of 100 pM probe DNA, the visible color changes (as shown in Figure 8, bottom) can be observed only after the addition of 10 nM complementary DNA, which indicates that our HRS assay is about two orders of magnitude more sensitive that the usual colorimetric technique.

After hybridization, the HRS intensity change can be due to several factors

1) Since aggregation takes place after hybridization, the nanorod loses the center of symmetry and, as a result, one can expect significant amount of electric-dipole contribution to the HRS intensity. Since electric dipole contributes several times higher than that of multipolar moments, we expect the HRS intensity to increase with aggregation.
2) When target DNA with complementary sequence is added to the probe DNA, a clear colorimetric change is observed due to the aggregation as shown in Figure 8 (top, absorption maximum changes from 697 to 950 nm). A two-level model that has been extensively used for donor–acceptor NLO chromophores can be used to explain the difference of first-order nonlinearity due to the change in color of nanorods. According to the two-state model,[42] Equation (2) can be written in which μ_{eg} is the

$$\beta^{\text{two state}} = \frac{3\mu_{eg}^2 \Delta\mu_{eg}}{E_{eg}^2} \frac{\omega_{eg}^2}{(1-4\omega^2/\omega_{eg}^2)(\omega_{eg}^2-\omega^2)} \qquad (2)$$

transition dipole moment between the ground state $|g\rangle$ and the charge-transfer excited state $|e\rangle$, $\Delta\mu_{eg}$ is the difference in dipole moment, and E_{eg} is the transition energy. As the color changes, the λ_{max} changes from 697 to 950 nm, β should change significantly and as a result HRS intensity changes.
3) The single photon resonance enhancement factor is much larger for nanorod aggregates due to the closeness of λ_{max} to the fundamental wavelength at 860 nm. This resonance enhancement should increase HRS intensity.
4) Since size increases significantly with aggregation, the HRS intensity should increase with the increase in particle size.

To understand how the HRS intensity increases with aggregation, we have performed HRS experiment on a pure gold nanorod solution with and without addition of NaCl.

Figure 9 shows how the HRS intensity increases with increasing NaCl concentration. Our experiment indicates that the HRS intensity is enhanced by a factor of 35 with respect to the HRS signal of the pure gold nanorod solution, then slightly decreases and finally saturates at a higher NaCl concentration. The enhancement factor is about the same for pure gold nanorods and DNA adsorbed gold nanorods after hybridization.

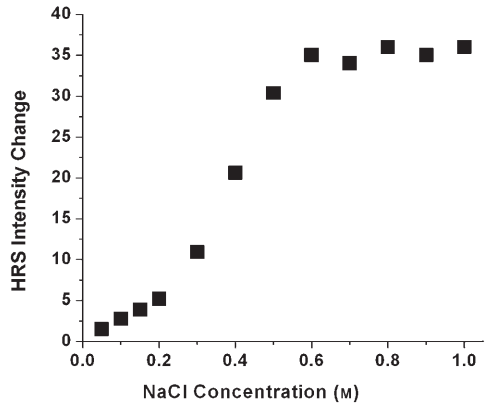

Figure 9. Plot of HRS intensity from god nanorod versus different concentration of NaCl.

For genomic analysis, it is desirable to detect specific sequences on much longer HIV DNA targets. To examine ability of our assays to quantify naturally occurring nucleic acid sequences, the HIV *gag* gene was used as a model system. Complementary DNA sequences matching a region found within the nucleocapsid portion of the HIV *gag* gene were tagged with gold nanorods and used as a probe.

Fragments containing 86, 115, 142, and 185 bp from the *gag* region of HIV-1 DNA was used as target. Figure 10 represents the results of proof-of-principle experiments for detecting matches to sequences on long targets; the only limitation is that the hybridization process is slow due to the slow adsorption process of long ss-DNA sequences on gold nanoparticles. Although large portions of the target remain single stranded and will presumably have the electrostatic properties of ss-DNA, we have no difficulty using the assay to determine whether these long targets contain sequences complementary to our short, dye-tagged probes. Thus, our technique is most practical when short, dye-tagged probes (≈45 mers) are used.

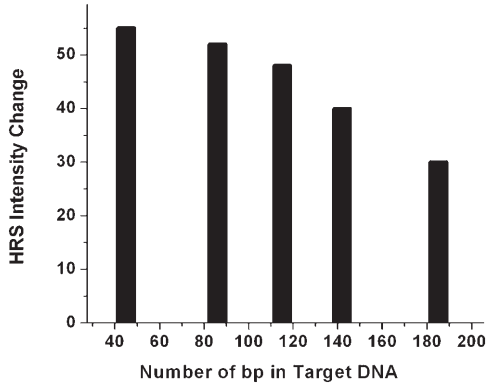

Figure 10. Plot of HRS intensity change as a function of number of base pairs of target *gag* region of HIV-1 DNA.

Conclusion

In conclusion, in this manuscript, we have demonstrated for the first time a label free, highly sensitive and sequence-specific HRS assay for HIV *gag* gene, DNA sequence recognition in 100 picomolar level. For a 145-mer oligonucletide probe, a 100 pM solution of target DNA can be detected with excellent discrimination against single-base mismatches. We provide experimental evidence for higher multipolar contribution to NLO response of gold nanorods. Our HRS assay have several advantages: 1) one can use unmodified protein and DNA to probe them in solution by the HRS technique, 2) it can be two orders of magnitude more sensitive than the usual colorimetric technique, and 3) single base-pair mismatches are easily detected. Our experimental results reported here open up a new possibility of rapid, easy, and reliable diagnosis of single-base-mismatch HIV-1 virus DNA by measuring the HRS intensity from DNA-modified gold nanorods. The methods and principles presented here can be applied to in-vitro-selected aptamers for recognizing a wide range of analytes such as small organic molecules and divalent cations. These nanorod-based HRS probes offer unique advantages and capabilities that are not available from traditional molecular systems. It is probably possible to improve the HRS intensity by several orders of magnitudes by choosing proper materials and detection systems.

Acknowledgement

Dr. Ray thanks NIH-SCORE (grant no. S06GM 008047), NSF-CRIFMU (grant no. 0443547), and NSF-PREM (grant no. DMR-0611539) for their generous funding.

[1] A. P. Alivisatos, *Nat. Biotechnol.* **2004**, *22*, 47–52.
[2] E. Katz, I. Willner, *Angew. Chem.* **2004**, *116*, 6166–6235; *Angew. Chem. Int. Ed.* **2004**, *43*, 6042–6108.
[3] J. Xiang, W. Lu, Y. Hu, Y. Wu, H. Yan, C. M. Lieber, *Nature* **2006**, *441*, 489.
[4] J. M. Nam, C. S. Thaxton, C. A. Mirkin, C. A. *Science* **2003**, *301*, 1884–1886.
[5] X. Gao, Y. Cui, R. M. Levenson, L. W. K. Chung, S. Nie, *Nat. Biotechnol.* **2004**, *22*, 969–976.
[6] P. C. Ray, *Angew. Chem.* **2006**, *118*, 1169–1172; *Angew. Chem. Int. Ed.* **2006**, *45*, 1151–1154.
[7] L.-Q. Chu, R. Förch, W. Knoll, *Angew. Chem.* **2007**, *119*, 5032–5035; *Angew. Chem. Int. Ed.* **2007**, *46*, 4944–4947.
[8] T. N. Grossmann, L Röglin, O Seitz, *Angew. Chem.* **2007**, *119*, 5315–5318; *Angew. Chem. Int. Ed.* **2007**, *46*, 5223–5226.
[9] X. Huang, I. H. El-Sayed, W. Qian, M. A. El-Sayed, *J. Am. Chem. Soc.* **2006**, *128*, 2115–2120.

[10] X. Huang, I. H. El-Sayed, W. Qian, M. A. El-Sayed, *Nano Lett.* **2007**, *7*, 1591–1597.
[11] G. H. Chan, J. Zhao, E. M. Hicks, G. C. Schatz, R. P. Van Duyne, *Nano Lett.* **2007**, *7*, 1947–1952.
[12] B. P. Khanal, E. R. Zubarev, *Angew. Chem.* **2007**, *119*, 2245–2248; *Angew. Chem. Int. Ed.* **2007**, *46*, 2195–2198.
[13] C.-C. Huang, Z. Yang, K.-H. Lee, H.-T. Chang, *Angew. Chem.* **2007**, *119*, 6948–6952; *Angew. Chem. Int. Ed.* **2007**, *46*, 6824–6828.
[14] P. C. Ray, A. Fortner, G. K. Darbha, *J. Phys. Chem. B.* **2006**, *110*, 20745–20748.
[15] T. L. Jennings, M. P. Singh, G. F. Strouse, *J. Am. Chem. Soc.* **2006**, *128*, 5462.
[16] P. C. Ray, G. K. Darbha, A. Ray, W. Hardy, *Nanotechnology* **2007**, *18*, 375504–375510.
[17] L. Fabris, M. Dante, G. Braun, S. J. Lee, N. O. Reich, M. Moskovits, T.-Q. Nguyen, G. C. Bazan, *J. Am. Chem. Soc.* **2007**, *129*, 6086–6087.
[18] S. Lal, N. K. Grady, G. P. Goodrich, N. J. Halas, *Nano Lett.* **2006**, *6*, 2338–2343.
[19] N. J. Durr, T. Larson, D. K. Smith, B. A. Korgel, K. Sokolov, A. B. Yakar, *Nano Lett.* **2007**, *7*, 941–945.
[20] S Satyabrata , T K. Mandal, *Chem. Eur. J.* **2007**, *13*, 3160–3168.
[21] J. Strzalka, T. Xu, A. Tronin, S. P. Wu, I. Miloradovic, I. Kuzmenko, T. Gog, M. J. Therien, J. K. Blasie, *Nano Lett.* **2006**, *6*, 2395–2405.
[22] I. Russier-Antoine, E. Benichou, G. Bachelier, C. Jonin, P. F. Brevet, *J. Phys. Chem. C* **2007**, *111*, 9044–9048.
[23] K. Clays, A. Persoons, *Phys. Rev. Lett.* **1991**, *66*, 2980–2983.
[24] G. Hennrich, M. T. Murillo, P. Prados, H. Al-Saraierh, A. El-Dali, D. W. Thompson, J. Collins, P. E. Georghiou, A. Teshome, I. Asselberghs, K. Clays, *Chem. Eur. J.* **2007**, *13*, 7753–7761.
[25] S. Kujala, B. K. Canfield, M. Kauranen, *Phys. Rev. Lett.* **2007**, *98*, 167403–167406.
[26] B. J. Coe, J. A. Harris, L. A. Jones, B. S. Brunschwig, K. Song, K. Clays, J. Garin, J. Orduna, S. J. Coles, M. B. Hursthouse, *J. Am. Chem. Soc.* **2005**, *127*, 4845–4859.
[27] L. Viau, S. Bidault, O. Maury, S. Brasselet, I. Ledoux, J. Zyss, E. Ishow, K. Nakatani, H. Le Bozec, *J. Am. Chem. Soc.* **2004**, *126*, 8386–8387.
[28] C. A. Mirkin, R. L. Letsinger, R. C. Mucic, J. J. Storhoff, *Nature* **1996**, *382*, 607–610.
[29] N. J. Durr, T. Larson, D. K. Smith, B. A. Korgel, K. Sokolov, A. Ben-Yakar, *Nano Lett.* **2007**, *7*, 941–945.
[30] C. Sonnichsen, A. P. Alivisatos, *Nano Lett.* **2005**, *5*, 301–304.
[31] P. K. Jain, S. K. Lee, I. H. El-Sayed, M. A. El-Sayed, *J. Phys. Chem. B.* **2006**, *110*, 7238–7248.
[32] H. F. Wang, T. B. Huff, D. A. Zweifel, W. He, P. S. Low, A. Wei, J.-X. Cheng, *Proc. Natl. Acad. Sci. USA* **2005**, *102*, 15752–15756.
[33] T. Yamada, Y. Iwasaki, H. Tada, H. Iwabuki, M. Chuah, T. Vanden-Driessche, H. Fukuda, A. Konodo, M. Ueda, M. Seno, K. Tanizawa, S. Kuroda, *Nat. Biotechnol.* **2003**, *21*, 885–890.
[34] C. J. Murphy, T. K. Sau, A. M. Gole, C. J. Orendroff, J. Gao, L. Gou, S. E. Hunyadi, T. Li, *J. Phys. Chem. B* **2005**, *109*, 13857–13870.
[35] G. K. Darbha, A. Ray, P. C. Ray, *ACS Nano* **2007**, *1*, 208–214.
[36] V. S. Tiwari, T. Oleg, G. K. Darbha, W. Hardy, J. P. Singh, P. C. Ray, *Chem. Phys. Lett.* **2007**, *446*, 77–82.
[37] H. Kang, G. Evmenenko, P. Dutta, K. Clays, K. Song, T. J. Marks, *J. Am. Chem. Soc.* **2006**, *128*, 6194–6205.
[38] P. Galletto, P. F. Brevet, H. H. Girault, R. Antoine, M. Broyer, *J. Phys. Chem. B* **1999**, *103*, 8706–8710.
[39] J. P. Novak, L. C. Brousseau, F. W. Vance, R. C. Johnson, B. I. Lemon, J. T. Hupp, D. L. Feldheim, *J. Am. Chem. Soc.* **2000**, *122*, 12029–12030.
[40] C. Hubert, A. Rumyantseva, G. Lerondel, J. Grand, S. Kostcheev, L. Billot, A. Vial, R. Bachelot, P. Royer, S.-H. Chang, S. K. Gray, G. P. Wiederrecht, G. C. Schatz, *Nano Lett.* **2005**, *5*, 615–619.
[41] G. Mie, *Ann. Phys.* **1908**, *25*, 377.
[42] J. L. Oudar, *J. Chem. Phys.* **1977**, *67*, 446–454.

Received: November 25, 2007
Published online: March 17, 2008

